

# Synthesis and multi-stimuli-responsive behavior of copolymer of $N,N'$ -dimethylacrylamide and complex pseudorotaxane

Hui Yang · Qiang Ma · Lin Hu · Jingcheng Hao · Yebang Tan

Received: 1 December 2011 / Revised: 14 February 2012 / Accepted: 29 February 2012 /  
Published online: 11 March 2012  
© Springer-Verlag 2012

**Abstract** Novel water-soluble side-chain copolymer with the pseudorotaxane structure threaded by cucurbit[6]uril (CB[6]) was synthesized by  $N'$ -(4-vinylbenzyl)-1,4-diaminobutane dihydrochloride with CB[6] threaded (4VBCB) and  $N,N'$ -dimethylacrylamide (DMAA) as monomers. SEM results show that the diameter of the spherical particles increases and the crosslinking in spherical particles occurred with the decrease of the molar ratio of DMAA/4VBCB. Interestingly,  $^1\text{H}$  NMR spectra show that the threading and dethreading of CB[6] on the side chains could be controlled by the addition of  $\text{CaCl}_2$  or  $\text{BaCl}_2$ , but CB[6] cannot drop from the side chains by the addition of NaCl. DLS data indicate that the copolymers have thermal sensitivity and their jump temperature could be controlled by adjusting the molar ratio of DMAA/4VBCB, and RLS data show that the size of aggregation increases with increasing the concentration of NaCl. At the same time, the copolymers have pH-responsive behavior.

**Keywords** Rotaxane · Cucurbit[6]uril · Self-assembly · Water-soluble polymer

## Introduction

Supramolecular polymers [1, 2] are inherently dynamic in nature and highly selective toward other complementary guest molecules due to these various weak

---

H. Yang · Q. Ma · L. Hu · Y. Tan (✉)  
School of Chemistry and Chemical Engineering, Shandong University, Jinan 250100,  
People's Republic of China  
e-mail: ybtan@sdu.edu.cn

J. Hao  
The Key Laboratory of Colloid and Interface Chemistry, Shandong University,  
Ministry of Education, Jinan 250100, People's Republic of China

Y. Tan  
Key Laboratory of Special Functional Aggregated Materials, Shandong University,  
Ministry of Education, Jinan 250100, People's Republic of China

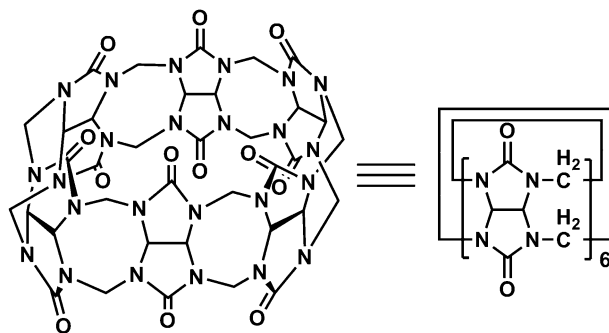


**Fig. 1** Structure of CB[6]

and reversible non-covalent interactions such as hydrogen bonding, ion–ion,  $\pi$ – $\pi$  stacking, and van der Waals interactions, and supramolecular systems could be engineered to assemble and disassemble spontaneously in response to a range of triggers because of their inherent modularity and reversibility [3–28].

Cucurbit[6]uril (CB[6]), a barrel-shaped host, consists of 6 glycoluril groups and 12 methylene bridges at both ends as shown in Fig. 1. The two rims are formed by the glycoluril carbonyl oxygen, thereby are negatively charged, and they develop ion–dipole interactions with cationic guests [29, 30]. Recently, taking advantage of cucurbit[*n*]uril's structure, various mechanically interlocked molecules including rotaxanes and poly(pseudo)rotaxanes have been synthesized by Kim [30–47], Buschman [48–51], and others [28, 52–62]. We previously synthesized some side-chain polypseudorotaxanes with cucurbit[*n*]uril as molecular bead have been also reported [63–69].

Poly(*N,N'*-dimethylacrylamide) (PDMAA) has temperature responsiveness, which have attracted extensive attention as water-absorbing, soft, and stimuli-sensitive materials [70–73]. Therefore, it is expected that the copolymer with DMAA and *N'*-(4-vinylbenzyl)-1,4-diaminobutane dihydrochloride with CB[6] threaded (4VBCB) can be synthesized. It is also expected that copolymer has more unique and complicated stimulation-responsive behaviors.

Herein, we synthesized novel water-soluble side-chain copolymer by 4VBCB and DMAA as monomers. The pH and thermo-responsive behavior of the copolymer was studied by DLS and RLS. At the same time, the stimuli-responsive behavior of salts for the copolymer was investigated by  $^1\text{H}$  NMR.

## Experimental

### Materials

CB[6] was prepared according to the literatures [29, 30]. *N'*-(4-vinylbenzyl)-1,4-diaminobutane dihydrochloride (4VB) was prepared according to the literature [66]. DMAA were received from Acros. Anhydrous acetonitrile (AR) and diethyl ether anhydrous (AR) were received from the Sinopharm Chemical Reagent Co., Ltd

(SCRC). Potassium persulfate (KPS, Acros) was recrystallized from the deionized water before use. Other chemicals were of reagent grade and used without further purification.

#### Synthesis of complex polypseudorotaxane monomer with CB[6] (4VBCB)

4VB (0.735 g, 3 mmol) was dissolved in deionized water (30 mL), and stirred for 10 min at room temperature. CB[6] (3.28 g, 3.3 mmol) was slowly added into the solution of 4VB, and the mixture was stirred for 24 h at room temperature. The reaction solution was filtrated and concentrated by rotary evaporation method, and precipitated by absolute ethyl alcohol. The white precipitate was purified with diethyl ether anhydrous and dried in vacuum to give 4VBCB (3.43 g, 92 %).  $^1\text{H}$  NMR (400 MHz,  $\text{D}_2\text{O}$ , ppm)  $\delta$ : 0.55 (s,  $\text{CH}_2\text{CH}_2\text{CH}_2\text{CH}_2$ , 4H), 2.26 (t,  $\text{CH}_2\text{CH}_2\text{CH}_2\text{CH}_2\text{NH}_2^+$ , 2H), 2.38 (t,  $\text{CH}_2\text{NH}_3^+$ , 2H), 5.33 (d,  $\text{PhCH}_2\text{NH}_2^+$ , 2H), 5.89 (d,  $\text{CH}_2=\text{CH}$ , 2H), 3.79 (m,  $\text{CH}_2=\text{CH}$ , H), 7.57 and 7.72 (d, Ph, 4H), 4.32 (d, 12H from CB[6]), 5.59 (s, 12H from CB[6]), 5.68 (d, 12H from CB[6]); IR (KBr,  $\text{cm}^{-1}$ )  $\nu$ : 1639 (C–N $^+$ ), 1731 (C=O of CB[6]); Anal. calcd for  $\text{C}_{49}\text{H}_{58}\text{N}_{26}\text{O}_{12}\text{Cl}_2$ : C 46.19, H 4.56, N 28.59; found C 45.94, H 4.81, N 28.43.

#### Synthesis of the water-soluble copolymer (P4VBCB/DMAA)

$\text{H}_2\text{O}$  (50 mL), DMAA (0.215 g, 0.0025 mol), and 4VBCB (1.243 g, 0.001 mol) were added into three-necked flask and stirred with a magnetic stir bar under an inert  $\text{N}_2$  atmosphere, and then heated to 85 °C with an oil bath. After thermal equilibrium had been reached and the solution had been bubbled for 0.5 h,  $\text{K}_2\text{S}_2\text{O}_8$  was added and reacted for 24 h at this temperature. The reaction aqueous was concentrated and precipitated with acetone and dried in vacuum to give the copolymer P4VBCB/DMAA-1 (1.38 g, 94 %). The solid power of PDMAA and the copolymers with different molar ratios of DMAA/4VBCB (P4VBCB/DMAA-2 and P4VBCB/DMAA-3) for the measurement of  $^1\text{H}$  NMR, DLS, RLS, and EA were synthesized by the above method as shown in Table 1.  $^1\text{H}$  NMR ( $\text{D}_2\text{O}$ , 400 MHz, ppm)  $\delta$ : 0.59 ( $\text{CH}_2\text{CH}_2\text{CH}_2\text{CH}_2$ ), 1.45 and 1.60 ( $\text{CH}_2$  and  $\text{CH}$  from the main chain of copolymer), 2.30 ( $\text{CH}_2\text{CH}_2\text{CH}_2\text{CH}_2\text{NH}_2^+$ ), 2.42 ( $\text{CH}_2\text{NH}_3^+$ ), 3.00 ( $\text{CH}_3$  from DMAA), 5.55 ( $\text{PhCH}_2\text{NH}_2^+$ ), 7.52 and 7.79 (Ph), 4.36 (12H from CB[6]), 5.66 (12H from CB[6]), 5.74 (12H from CB[6]); IR (KBr,  $\text{cm}^{-1}$ )  $\nu$ : 1633 (C–N $^+$ ), 1447 (C=C from phenyl), 1731 (C=O of CB[6]).

#### Characterization

All  $^1\text{H}$  NMR experiments were performed on a Bruker AVANCE400 NMR spectrometer.  $\text{D}_2\text{O}$  was used for field-frequency lock, and the observed  $^1\text{H}$  chemical shifts were reported in parts per million (ppm) relative to an internal standard (TMS, 0 ppm).

FT-IR was carried out on a Tensor 27 spectrometer (Bruker, Switzerland) with sample prepared as KBr pellets. The spectra were acquired in the frequency range 4,000–400  $\text{cm}^{-1}$  at a resolution of 4  $\text{cm}^{-1}$  with a total of 16 scans.

**Table 1** Copolymer composition and the weight-average molar mass  $M_w$  of P4VBCB/DMAA and PDMAA

Sample	Feed molar ratio of DMAA/4VBCB	Elemental analysis			Actual molar ratio of DMAA/4VBCB <sup>a</sup>	$M_w$ (g/mol) <sup>b</sup>
		C (wt%)	H (wt%)	N (wt%)		
PDMAA	–	60.61	9.09	14.14	–	$5.18 \times 10$
PDMAA/4VBCB-1	2.5	48.53	5.30	26.24	2.4	$8.19 \times 10$
PDMAA/4VBCB-2	4.0	50.18	5.68	25.55	4.0	$6.61 \times 10$
PDMAA/4VBCB-3	5.5	50.39	5.88	24.25	5.4	$5.78 \times 10$

<sup>a</sup> Determined by <sup>1</sup>H NMR spectra

<sup>b</sup> Determined by static light scattering

Elemental analyses (C, N, and H) were performed on Elementar Vario E1 III analyzer (German).

Multi-angle laser light scattering (MALLS) measurements were performed by the Wyatt Technology DAWN HELEOS 18 angle (from 15° to 165°) light scattering detector using a Ga–As laser (658 nm, 40 mW). The refractive index increments ( $dn/dc$ ) of P4VBCB/DMAA in aqueous solution were determined at 25 °C by an Optilab Rex interferometric refractometer (Wyatt Technology) at the wavelength of 658 nm, and the concentrations of P4VBCB/DMAA determined in the solution of 0.1 mol/L NaCl for Zimm plot were  $5 \times 10^{-5}$ ,  $1.5 \times 10^{-4}$ ,  $2.5 \times 10^{-4}$ ,  $3.5 \times 10^{-4}$ , and  $4.5 \times 10^{-4}$  g/mL.

DLS measurements were performed on Dawn Heleos, Wyatt QELS, and Optilab DSP instruments. The water used for light scattering measurements was all filtered through 0.22- $\mu$ m hydrophilic membranes (Millipore) before using. Solutions were prepared by the weighing method. Stock solutions were prepared by dissolving the copolymers in aqueous solution in volumetric flasks. Solutions with different concentrations were prepared for light scattering measurements by diluting the stock solutions.

The RLS measurement was performed at room temperature on a Hitachi F-4500 fluorescence spectrophotometer (Tokyo, Japan). The slit (ex/em) width was 5 nm/5 nm. The excitation and emission spectra were recorded in range of 250–500 nm with synchronous at  $\lambda_{ex} = \lambda_{em}$  (i.e.,  $\Delta\lambda = 0$  nm) according to the literature [76].

The morphologies of the copolymer were observed in scanning electron microscopy (SEM) (Qanta200ESEM FEIco-Holland) with an accelerating voltage of 20 kV.

Data of X-ray Powder Diffraction (XRD) were collected on a Max 2200PC power X-ray diffractometer (Rigaku, Japan) with Cu-K $\alpha$  (1.54051 Å) radiation (40 kV, 20 mA). Powder samples were mounted on a sample holder and scanned with a step size of  $2\theta = 0.02^\circ$  between  $2\theta = 5^\circ$  and  $50^\circ$ .

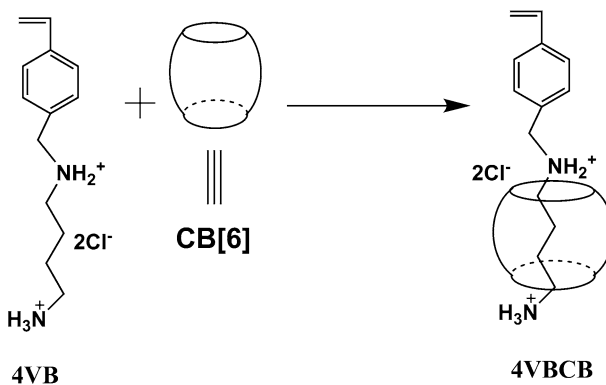
The pH experiments were performed on a pHs-3 type pH meter made in Shanghai Leici Instrument Company with the E-201-C type glass electrode. Conductivity experiments were performed on the E-201-C type glass electrode together with 232 type Hg electrode as a reference electrode.

## Results and discussion

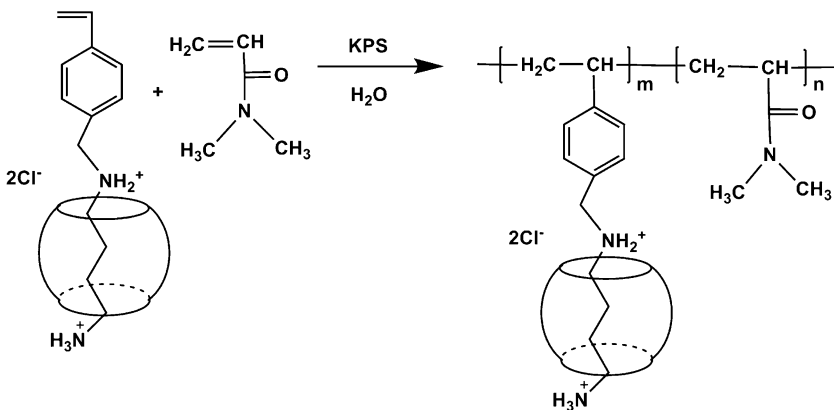
### Preparation of the pseudorotaxane monomer and P4VBCB/DMAA

The pseudorotaxane monomer (4VBCB) was easily achieved by self-assembly of 4VB with a certain amount of CB[6] in water at room temperature for 12 h as shown in Scheme 1. The copolymer P4VBCB/DMAA was prepared using  $K_2S_2O_8$  as the initiator and 4VBCB and DMAA as the monomers in water under the inter  $N_2$  atmosphere by the free radical polymerization as shown in Scheme 2.

PDMAA and the copolymers with different molar ratios of DMAA/4VBCB were determined by elemental analysis as shown in Table 1, while the actual molar ratio of DMAA/4VBCB calculated via  $^1H$  NMR spectra and the weight-average molar mass  $M_w$  of P4VBCB/DMAA and PDMAA are shown in Table 1.

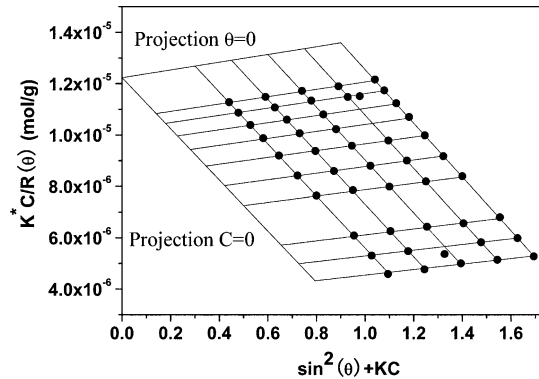


**Scheme 1** Synthesis of the pseudorotaxane monomer 4VBCB



**Scheme 2** Synthesis of P4VBCB/DMAA

**Fig. 2** Zimm plot for P4VBCB/DMAA-1 in 0.1 mol/L NaCl



In static light scattering, we are able to obtain the weight-average molar mass  $M_w$ , the second-order virial coefficient  $A_2$ , and the mean square radius  $\langle r_g^2 \rangle$  of polymer chains from the angular dependence of the excess absolute scattering intensity, known as the Rayleigh ratio  $R(\theta)$ , on the basis of

$$\frac{K^*C}{R(\theta)} = \frac{1}{M_w} \left( 1 + \frac{1}{3} \langle r_g^2 \rangle q^2 \right) + 2A_2C \quad (1)$$

where  $K^* = 4\pi(dn/dc)^2 n_0 / (N_A \lambda_0^4)$ , and  $q = (4\pi n_0 / \lambda_0) \sin(\theta/2)$ , with  $n_0$ ,  $dn/dc$ ,  $\lambda_0$ , and  $\theta$  being the solvent refractive index, the specific refractive index increment, the wavelength of the incident light in vacuum, and the scattering angle, respectively [74, 75]. Figure 2 shows a static Zimm plot of P4VBCB/DMAA-1 in solution of 0.1 mol/L NaCl, where  $C$  ranges from  $5.0 \times 10^{-5}$  to  $4.5 \times 10^{-4}$  g/mL. The date of static light scattering measurements indicate that the weight-average molar mass  $M_w$  of P4VBCB/DMAA-1 was  $8.19 \times 10^4$  g/mol, and the  $M_w$  of PDMAA and copolymers with different molar ratios of 4VBCB to DMAA were determined by static light scattering as shown in Table 1.

### $^1\text{H}$ NMR spectra

The formation of copolymers was confirmed by  $^1\text{H}$  NMR spectrum. Figure 3 was the  $^1\text{H}$  NMR spectrum of 4VB and pseudorotaxane monomer 4VBCB. It reveals that upon formation of the complex, signals appear at 5.74, 5.66, and 4.36 ppm, which correspond to threaded CB[6]. The methylene proton signals of the butyl diamine units of 4VB (peaks 7, 8, 9, and 10) are upfield shifted, and the methylene proton signals of benzyl units of 4VB (peak 6) is downfield shifted due to the shielding effect of CB[6] [65, 66]. The  $^1\text{H}$  NMR data support that CB[6] beads threaded on 4VB are localized on the butyl diamine units, and the molar ratio of CB[6] to 4VB is 1:1. The high threading efficiency is due to the multiple non-covalent interactions between the positively charged nitrogen atoms of protonated butyl diamine and the CB[6] portal oxygen atoms, and the resulting complex pseudorotaxane is quite stable in solution and solid state.

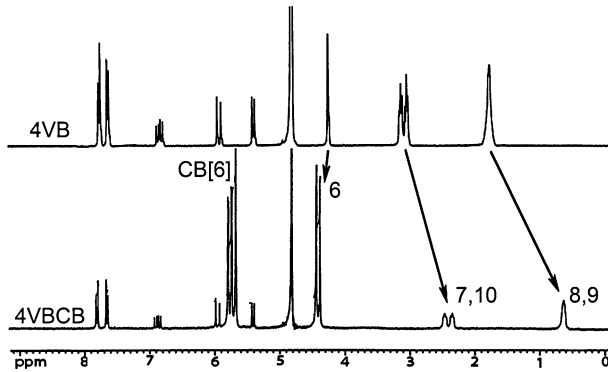


**Fig. 3**  $^1\text{H}$  NMR spectra of 4VB and 4VBCB

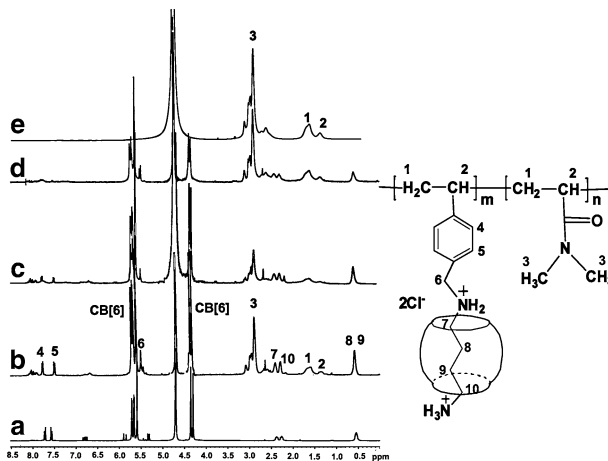
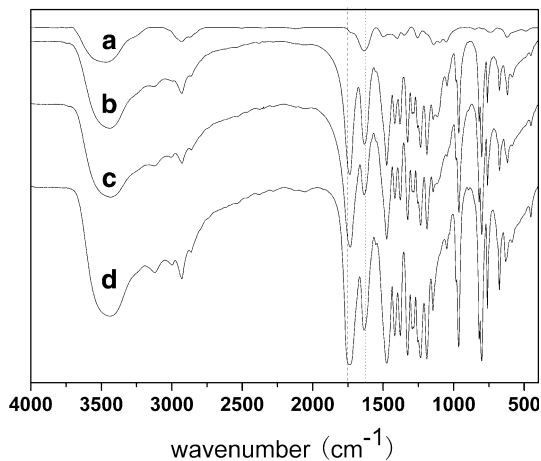


**Fig. 4**  $^1\text{H}$  NMR spectra of 4VBCB (a), PDMAA (e), and copolymer with CB[6]: (d) P4VBCB/DMAA-1, (c) P4VBCB/DMAA-2, (b) P4VBCB/DMAA-3

Figure 4b–e are the  $^1\text{H}$  NMR spectra of PDMAA and copolymer with CB[6]. Figure 4b–e shows that no peaks corresponding to  $-\text{CH}=\text{CH}_2$  are observed in the  $^1\text{H}$  NMR spectrum. Comparing with the  $^1\text{H}$  NMR spectrum of PDMAA (e), new broad signals appear at 4.36, 5.66, and 5.74 ppm, which correspond to the threading CB[6], and the methyl signals of DMAA at 3.00 ppm are also observed in the  $^1\text{H}$  NMR spectrum of Fig. 4b–d. At the same time, the ratio of the area of peak 3 (the methyl signals of DMAA) to the peaks 8 and 9 (the methylene signals of 4VBCB shielded by CB[6]) increases with the increase of the molar ratio of DMAA/4VBCB. All these data were consistent with the fact that CB[6] beads are localized on the butyl diammonium units of the side chains, and it did not shed from the side chains of copolymer after the polymerizations. The results of molar ratio of DMAA/4VBCB were calculated from the ratio of the integrals areas between the signals of peaks 3, 8, and 9 as listed in Table 1.

**Fig. 5** FT-IR spectra of PDMAA (a) and copolymer with CB[6]: (b) P4VBCB/DMAA-1, (c) P4VBCB/DMAA-2, (d) P4VBCB/DMAA-3



### FT-IR spectra

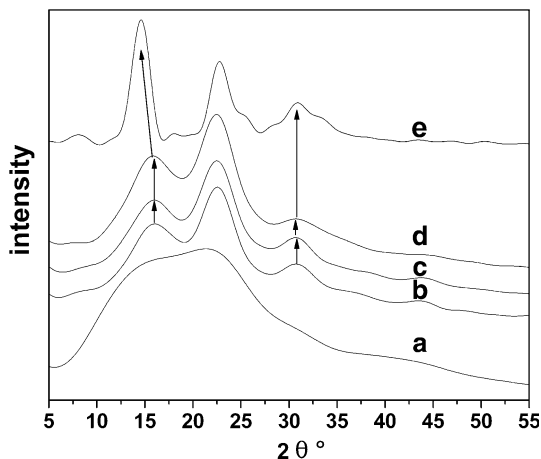
Figure 5 shows FT-IR spectra of PDMAA, copolymer with CB[6] P4VBCB/DMAA with different molar ratios of DMAA/4VBCB. The carbonyl moiety of DMAA is denoted by absorption at  $1,637\text{ cm}^{-1}$  as shown in Fig. 5a–d. Compared with the carbonyl moiety of DMAA, the carboxyl group absorption peak of CB[6] was observed at  $1,750\text{ cm}^{-1}$  in the curves of b, c, and d of Fig. 5. The band at  $1,475\text{ cm}^{-1}$  corresponds to the stretching frequency of C=N in the CB[6], and the rocking vibration of  $\text{CH}_2$  in CB[6] was observed at  $802\text{ cm}^{-1}$ . The ratio of intensity of the peaks at  $1,637\text{--}1,750\text{ cm}^{-1}$  increase gradually with increasing the molar ratio of DMAA/4VBCB as shown in Fig. 5b–d. The FT-IR results consistent with that of the  $^1\text{H}$  NMR spectra.

### X-ray powder diffraction (XRD)

Figure 6 shows the XRD patterns of PDMAA, copolymers with different molar ratios of DMAA/4VBCB and CB[6]. No sharp peaks reflected in the pattern of PDMAA show that it is a typical non-crystalline polymer as shown in Fig. 6a, while CB[6], comparing with PDMAA, has crystal composition because there are three sharper peaks ( $2\theta = 14.8^\circ, 23.2^\circ, 31.2^\circ$ ) in the XRD pattern in Fig. 6e. While comparing with PDMAA, copolymers with different molar ratios of DMAA/4VBCB have crystal composition because there are three sharper peaks ( $2\theta = 16.0^\circ, 22.6^\circ, 30.8^\circ$ ) in the XRD pattern and approach that of pure CB[6] as shown in Fig. 6b–d. As the molar ratio of DMAA/4VBCB increases from 2.5 to 5.4 as shown in Fig. 6b–d, the intensity of the peaks ( $2\theta = 16.0^\circ, 22.6^\circ, 30.8^\circ$ ) decrease with increasing molar ratio of DMAA/4VBCB as shown in Fig. 6. The decreasing intensity suggests that the threading of CB[6] on the side chains of copolymer may cause chain conformational changes of the copolymer. Compared with the parent PDMAA, the copolymers with the structure of pseudorotaxane have more regular chain conformation because of



**Fig. 6** The XRD curves of PDMAA (a) and copolymers with CB[6]: (b) P4VBCB/DMAA-1, (c) P4VBCB/DMAA-2, (d) P4VBCB/DMAA-3, (e) CB[6]



amount of the threading CB[6] beads, and the regularity of the chain conformation increases with increasing amount of the threading CB[6].

#### Scanning electron microscopy (SEM)

The morphology of the copolymers with different molar ratios of DMAA/4VBCB was investigated by SEM as shown in Fig. 7. The surface of copolymers with different molar ratios of DMAA/4VBCB shows a series of spherical particles with different diameters. At the same time, the SEM images show that the diameter of the spherical particles increases with the decrease of the molar ratio of DMAA/4VBCB because that with the addition of 4VBCB, the random chains of polymer are taken on a structure of a nearly circle with the beads of CB[6] lies out the circle, which are attributed to the bulky steric hindrance of CB[6]. So, the copolymers with the structure of pseudorotaxane have more regular chain conformation with decreasing the molar ratio of DMAA/4VBCB as the result of the XRD. The results of SEM research show that the introduction of the pseudorotaxane monomer in the copolymer could cause chain conformational changes.

#### The stimuli-responsive behavior of salts for the copolymer

The two rims of CB[6] are formed by the glycoluril carbonyl oxygen, thereby are negatively charged, so they develop strong ion–dipole interactions with cationic guests. For example, the binding constant of CB[6] with  $\text{Ba}^{2+}$  is  $1.7 \times 10^5$  L/mol [49], and the binding constant of CB[6] with  $\text{Ca}^{2+}$  is  $3.7 \times 10^4$  L/mol [77]. So, the proper  $\text{Ba}^{2+}$  or  $\text{Ca}^{2+}$  was added into the solution of P4VBCB/DMAA-1, which leads to that CB[6] could shed from the pseudorotaxane structure in the side chains of copolymer, and the copolymer with quaternary ammonium salts could be free. It provides theoretical basis for the application of the copolymer with the pseudorotaxane structure in drug release because the quaternary ammonium salt shielded by CB[6] is non-toxic compared with the physiological toxicity of the free quaternary

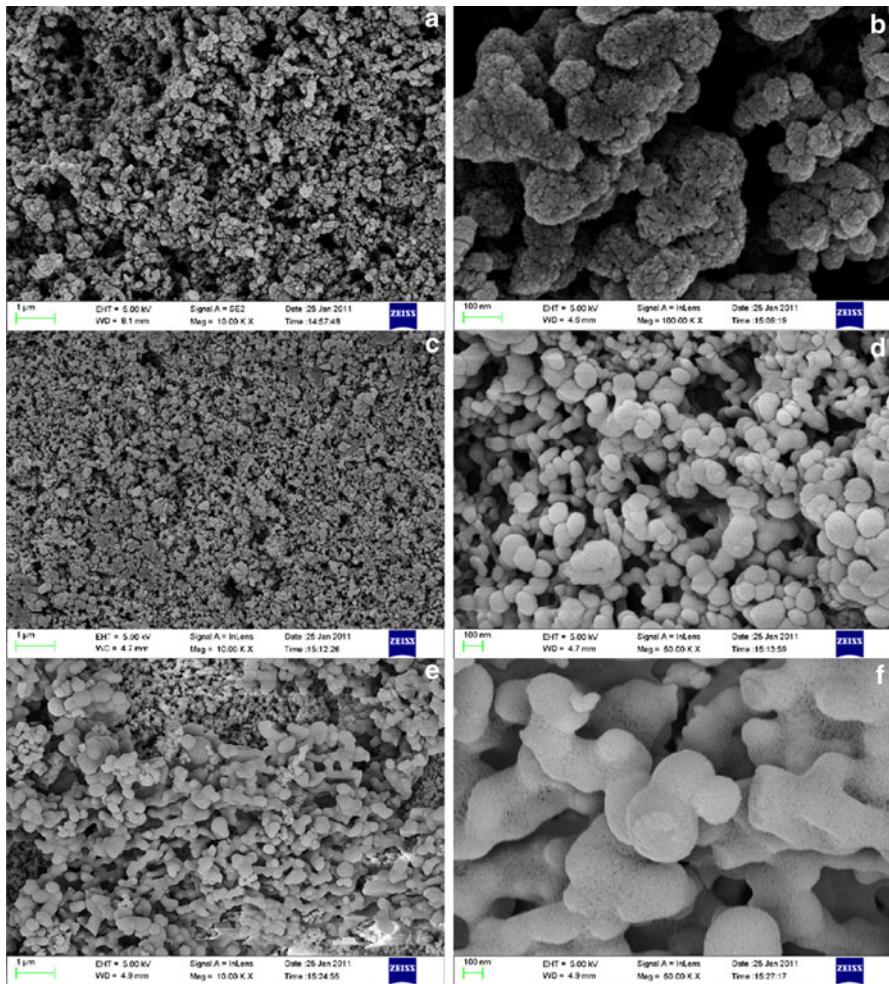


**Fig. 7** SEM images of copolymer with CB[6]: **a, b** P4VBCB/DMAA-3; **c, d** P4VBCB/DMAA-2; **e, f** P4VBCB/DMAA-1

ammonium salt. Figure 8 shows the  $^1\text{H}$  NMR spectra of P4VBCB/DMAA-1 (a), P4VBCB/DMAA-1 with the addition of  $\text{BaCl}_2$  (c) or  $\text{CaCl}_2$  (b), and  $\text{NaCl}$  (d). P4VBCB/DMAA-1 (10 mg) was added into the solution of  $\text{CaCl}_2$  (0.1 mol/L). The methylene signals of 4VB in the side chains shifts lowfield as shown in Fig. 8a, b, which indicates that CB[6] could shed from the pseudorotaxane structure in the side chains of copolymer with the addition of  $\text{CaCl}_2$ . At the same time, P4VBCB/DMAA-1 (10 mg) was also added into the solution of  $\text{BaCl}_2$  (0.1 mol/L), and Fig. 8a, c shows that the methylene signals of 4VB in the side chains shifts lowfield to 1.7 ppm and the proton signals of CB[6] disappear. It is indicated that CB[6] could also shed from the pseudorotaxane structure in the side chains of copolymer with the addition of  $\text{BaCl}_2$ . But P4VBCB/DMAA-1 (10 mg) was also added into the

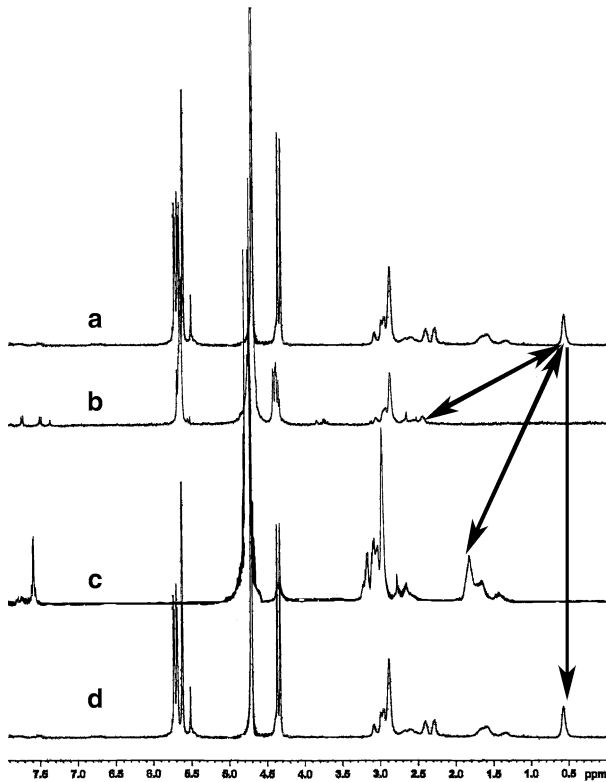


**Fig. 8**  $^1\text{H}$  NMR spectra of P4VBCB/DMAA-1 (a), P4VBCB/DMAA-1 with the addition of  $\text{BaCl}_2$  (c) or  $\text{CaCl}_2$  (b), and  $\text{NaCl}$  (d)

solution of  $\text{NaCl}$  (0.2 mol/L), and Fig. 8a, d shows that the methylene signals of 4VB could not shift and the proton signals of CB[6] could not disappear comparing the addition  $\text{CaCl}_2$  or  $\text{BaCl}_2$ . It suggests that the addition of  $\text{NaCl}$  could not have effect on the dethreading of CB[6] from the side chains of copolymer, which may be because of the binding constant of CB[6] with  $\text{Na}^+$ . The difference of the  $^1\text{H}$  NMR spectra of P4VBCB/DMAA-1 with adding  $\text{CaCl}_2$  or  $\text{BaCl}_2$  may be due to the binding constant of CB[6] with  $\text{Ca}^{2+}$  or  $\text{Ba}^{2+}$ . If the  $\text{Ba}^{2+}$  or  $\text{Ca}^{2+}$  could be removed as precipitate, CB[6] could thread on the side chains again. So,  $\text{Na}_2\text{CO}_3$  or  $\text{Na}_2\text{SO}_4$  was added into the  $\text{CaCl}_2$  or  $\text{BaCl}_2$  solution of P4VBCB/DMAA-1 for the removal of  $\text{Ca}^{2+}$  or  $\text{Ba}^{2+}$ . As expected, CB[6] could thread on the side chains again as shown in Fig. 8a. All the above experimental was repeated three times to prove the reversibility of threading and dethreading of CB[6] in the side chains of copolymer with the pseudorotaxane structure with the addition of  $\text{Ca}^{2+}$  or  $\text{Ba}^{2+}$ . The experimental results consistent with Fig. 8, so threading and dethreading of CB[6] in the side chains could be controlled by the addition of salts as shown in Fig. 9.

$\text{NaCl}$  has no effect on the threading and dethreading of CB[6] from the side chains, so the effect of  $\text{NaCl}$  on the aggregation behavior of the copolymer could be

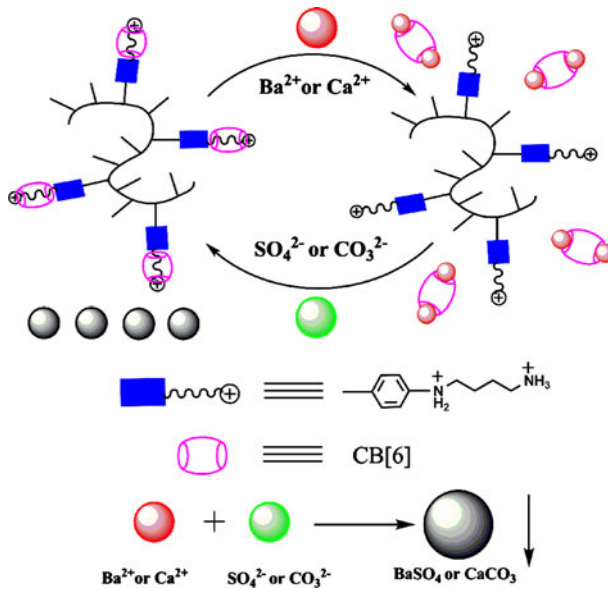


**Fig. 9** The schematic illustration of threading and dethreading of CB[6] from the side chains by the addition of salts

studied by RLS, because RLS is extremely sensitive and selective in probing the aggregation of the molecular chains [76]. Figure 10 shows the RLS spectra of P4VBCB/DMAA-1 (0.2 mg/mL) at different concentrations of the NaCl solution. The maximum scattering wavelengths ( $\lambda_{\text{max}}$ ) are about 394 nm, and other smaller scattering peaking at 354, 455, and 530 nm. The four peaks are the RLS information of P4VBCB/DMAA-1, and considering the sensitivity of detection, the maximum scattering wavelength (394 nm) was selected for further work. The RLS intensity at 394 nm increases with increasing concentration of the NaCl solution from 0.1 to 0.8 mol/L, which indicates that the sizes of the aggregation of copolymer with the pseudotaxanes structure increase with increasing the addition of NaCl. It is considered that CB[6] threaded on side chains could be shielded by  $\text{Na}^+$ , which leads to the electrostatic repulsive interaction of the side chains of copolymer decreases. So, the intermolecular interaction of copolymer enhances that result in the increase of the size of aggregation with increasing the concentration of NaCl.

#### Thermo-responsive behavior for the copolymer

The temperature responsiveness of DMAA is based on the balance of the hydrophilicity and hydrophobicity. Temperature responsiveness is caused by the hydrophobic interaction based on the hydration and dehydration of the methyl group of side chain [71]. Figure 11 shows the hydrodynamic radius distribution of P4VBCB/DMAA-3 (0.2 mg/mL) with increasing the temperature. The hydrodynamic radius of P4VBCB/DMAA-3 shifts to the large size with increasing the temperature from 25 to 45 °C, and the hydrodynamic radius distribution is broad at the high temperature as

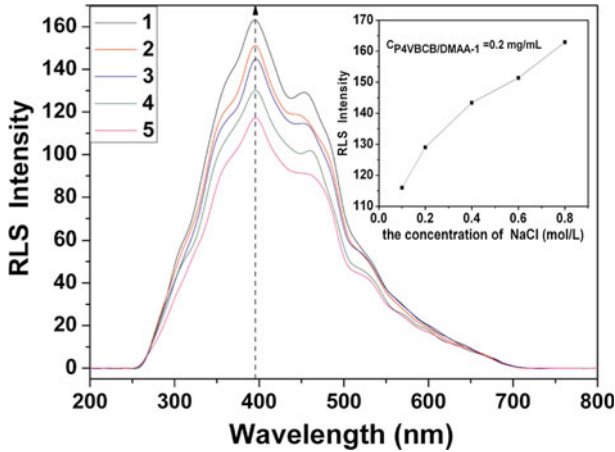


**Fig. 10** The RLS spectra of P4VBCB/DMAA-1 (0.2 mg/mL) at different concentrations of the NaCl solution: 1 0.8 mol/L, 2 0.6 mol/L, 3 0.4 mol/L, 4 0.2 mol/L, 5 0.1 mol/L

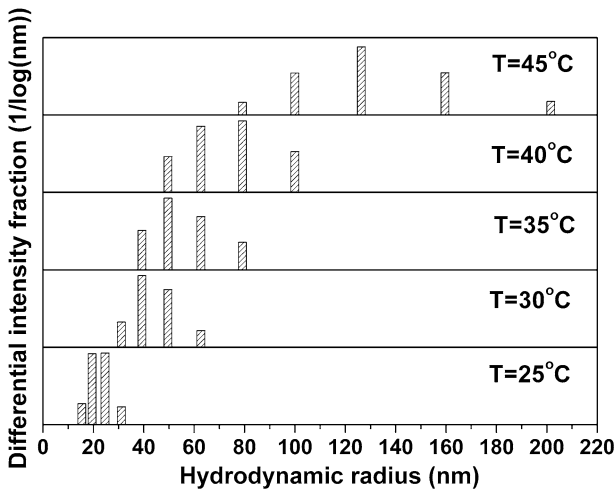
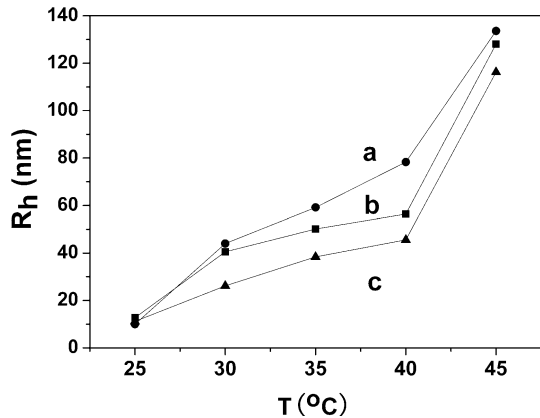


**Fig. 11** The effect of temperature on hydrodynamic radius distribution of P4VBCB/DMAA-3 (0.2 mg/mL)

shown in Fig. 11. It is indicated that the size of aggregation increases with the increase of temperature because of the hydrogen bonding interaction of nitrogen atoms of amide groups of DMAA unites with H<sub>2</sub>O [78–80]. When the temperature of the solution increases, the hydrogen bonding interaction of nitrogen atoms of amide groups of DMAA unites with H<sub>2</sub>O was destroyed, and the hydrophobic interaction of the two methyl groups of DMAA was enhanced and the molecular conformation of the copolymer was changed as shown in Fig. 14, which leads to the increase of the aggregation with increasing the temperature. Figure 12 shows the DLS curves of P4VBCB/DMAA (0.2 mg/mL) with different molar ratios of DMAA/4VBCB with

**Fig. 12** The effect of temperature on hydrodynamic radius of P4VBCB/DMAA (0.2 mg/mL) with different molar ratios of DMAA/4VBCB: (a) P4VBCB/DMAA-1, (b) P4VBCB/DMAA-2, (c) P4VBCB/DMAA-3



increasing the temperature. The hydrodynamic radius of P4VBCB/DMAA with different molar ratios of DMAA/4VBCB increases with increasing the temperature, and the jump temperature decreases with increasing the molar ratio of DMAA/4VBCB because that the enhanced rigidity and the bulky steric hindrance of side chains of P4VBCB/DMAA with the pseudorotaxanes structure threaded by CB[6] decrease with increasing the mole ratio of DMAA/4VBCB. It is indicated that the copolymer with the pseudorotaxanes structure has thermal sensitivity and their jump temperatures could be controlled by adjusting the molar ratio of DMAA/4VBCB in the copolymers.

#### The pH-responsive behavior for the copolymer

To study pH-responsive behavior of copolymer with the pseudorotaxanes structure, HCl (1 mol/L) was added into the solution of P4VBCB/DMAA at first, and the solution of NaOH (0.1 mol/L) was added dropwise into the acidic solution of P4VBCB/DMAA. At the same time, the pH of the solution of P4VBCB/DMAA was determined. Figure 13 shows that the effect of the concentration of NaOH on the pH of the solution of P4VBCB/DMAA. By adding the solution of NaOH (0.1 mol/L), pH of the solution of P4VBCB/DMAA has no change, but pH of the solution of P4VBCB/DMAA increases rapidly when the volume of NaOH added reaches to 0.85 mL, and then the pH keeps invariant after adding the volume of NaOH to 1.05 mL as shown in Fig. 13. It is considered that the added NaOH should first abstract  $H^+$  from protonated 1,4-diaminobutane moiety of copolymers to neutralize the P4VBCB/DMAA copolymers, and then the threading CB[6] are dethreading from the side chains. The jump of pH value clearly indicates the complete dethreading of the threading CB[6]. It is indicated that the copolymer with the pseudorotaxanes structure has pH-responsive behavior. And HCl solution was again added into the solution of P4VBCB/DMAA to test the reversibility of pH-responsive behavior of P4VBCB/DMAA aqueous solutions. The experimental results were consistent with Fig. 13, so threading and dethreading of CB[6] on the side chains could be controlled by adjusting pH of the copolymers as shown in Fig. 14.

**Fig. 13** The pH curves of the solution of P4VBCB/DMAA-1, P4VBCB/DMAA-2, P4VBCB/DMAA-3 (15 mL, 0.2 mg/mL) aqueous solution with adding the solution of NaOH (0.1 mol/L)

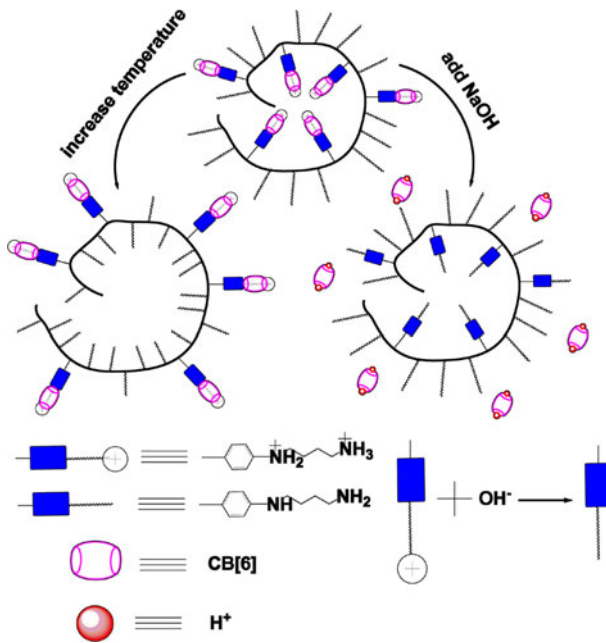
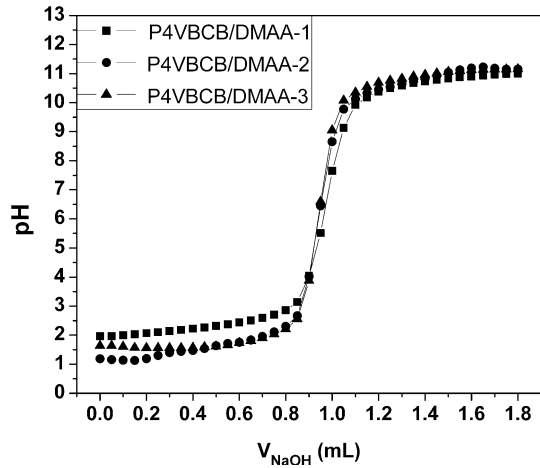


**Fig. 14** The schematic illustration of the pH and thermo-responsive behavior of copolymer

**Conclusions**

We synthesized novel water-soluble side-chain copolymer with the pseudorotaxanes structure, which could be threaded by CB[6] to 4VB. The introduction of the pseudorotaxane monomer in the copolymer could cause chain conformational changes, and threading and dethreading of CB[6] on the side chains could be controlled by the addition of CaCl<sub>2</sub> or BaCl<sub>2</sub>. Copolymers have thermal sensitivity

and their jump temperatures could be controlled by adjusting the molar ratio of DMAA/4VBCB in the copolymers, and the increase of the size of aggregation with increasing the concentration of NaCl. At the same time, the copolymer with the pseudorotaxanes structure has pH-responsive behavior.

**Acknowledgments** The authors are grateful for financial support from the National Natural Science Foundation of China (No. 20674045), National Basic Research Program of China (973 Program, 2009CB930103), and Shandong Provincial Natural Science Foundation (ZR2011BM002).

## References

1. Raymo FM, Stoddart JF (1999) Interlocked macromolecules. *Chem Rev* 99:1643
2. Lehn JM (1988) Supramolecular chemistry—scope and perspectives molecules, supermolecules, and molecular devices (nobel lecture). *Angew Chem Int Ed* 27:89
3. Gibson HW, Bheda MC, Engen PT (1994) Rotaxanes, catenanes, polyrotaxanes, polycatenanes and related materials. *Prog Polym Sci* 19:843
4. Amabilino DB, Stoddart JF (1995) Interlocked and intertwined structures and superstructures. *Chem Rev* 95:2725
5. Nepogodiev SA, Stoddart JF (1998) Cyclodextrin-based catenanes and rotaxanes. *Chem Rev* 98:1959
6. Balzani V, Gomez-Lopez M, Stoddart JF (1998) Molecular machines. *Acc Chem Res* 31:405
7. Chamborn J, Sauvage J (1998) Functional rotaxanes: from controlled molecular motions to electron transfer between chemically nonconnected chromophores. *Chem Eur J* 4:1362
8. Murakami H, Kawabuchi A, Kotoo K, Kunitake M, Nakashima N (1997) A light-driven molecular shuttle based on a rotaxane. *J Am Chem Soc* 119:7605
9. Bissell RA, Cordova E, Kaifer AE, Stoddart JF (1994) A chemically and electrochemically switchable molecular shuttle. *Nature* 369:133
10. Lane AS, Leigh DA, Murphy A (1997) Peptide-based molecular shuttles. *J Am Chem Soc* 119:11092
11. Jun SI, Lee JW, Sakamoto S, Yamaguchi K, Kim K (2000) Rotaxane-based molecular switch with fluorescence signaling. *Tetrahedron Lett* 41:471
12. Choi SW, Park SH, Ziganshina AY, Ko YH, Lee JW, Kim K (2003) A stable *cis*-stilbene derivative encapsulated in cucurbit[7]uril. *Chem Commun* 18:2176
13. Tuncel D, Steinke JHG (1999) Formation of oligotriazoles catalysed by cucurbituril. *Chem Commun* 16:1509
14. Tuncel D, Steinke JHG (2001) Mainchain pseudopolyrotaxanes via post-threading with cucurbituril. *Chem Commun* 3:253
15. Krasia TC, Steinke JHG (2002) Formation of oligotriazoles catalysed by cucurbituril. *Chem Commun* 1:22
16. Tuncel D, Steinke JHG (2004) Catalytic self-threading: a new route for the synthesis of polyrotaxanes. *Macromolecules* 37:288
17. Harada A, Li J, Kamachi M (1992) The molecular necklace: a rotaxane containing many threaded-cyclodextrins. *Nature* 356:325
18. Harada A, Li J, Kamachi M (1993) Macromolecular recognition. Formation of inclusion complexes of polymers with cyclodextrins. *Proc Jpn Acad Ser B* 69:39
19. Kamitori S, Matsuzaka O, Kondo S, Muraoka S, Okuyama K, Noguchi K, Okada M, Harada A (2000) A novel pseudo-polyrotaxane structure composed of cyclodextrins and a straight-chain polymer: crystal structures of inclusion complexes of  $\beta$ -cyclodextrin with poly(trimethylene oxide) and poly(propylene glycol). *Macromolecules* 33:1500
20. Herrmann W, Keller B, Wenz G (1997) Kinetics and thermodynamics of the inclusion of ionene-6, aqueous solution. *Macromolecules* 30:4966
21. Fujita H, Ooya T, Yui N (1999) Thermally induced localization of cyclodextrins in a polyrotaxane consisting of  $\beta$ -cyclodextrins and poly(ethylene glycol)-poly(propylene glycol) triblock-copolymer. *Macromolecules* 32:2534
22. Harada A, Okada M, Kawaguchi Y, Kamachi M (1999) Macromolecular recognition: new cyclodextrin polyrotaxanes and molecular tubes. *Polym Adv Technol* 10:3



23. Hodge P, Monvisade P, Owen GJ, Heatley F, Pang Y (2000)  $^1\text{H}$  NMR spectroscopic studies of the structures of a series of pseudopolyrotaxanes formed by “threading”. *New J Chem* 24:703
24. Gong CG, Ji Q, Subramaniam C, Gibson HW (1998) Main chain polyrotaxanes by threading crown ethers onto a preformed polyurethane: preparation and properties. *Macromolecules* 31:1814
25. Mason PE, Bryant WS, Gibson HW (1999) Dethreading exchange rates as structural probes in polypseudorotaxanes. *Macromolecules* 32:1559
26. Takata T, Kihara N, Furusho Y (2004) Polyrotaxanes and polycatenanes: recent advances in syntheses and applications of polymers comprising of interlocked structures. *Adv Polym Sci* 171:1
27. Huang F, Gibson HW (2005) Polypseudorotaxanes and polyrotaxanes. *Prog Polym Sci* 30:982
28. Harada A, Hashizume A, Yamaguchi H, Takashima Y (2009) Polymeric rotaxanes. *Chem Rev* 109:5974
29. Day A, Arnold AP, Blanch RJ, Snushall BJ (2001) Controlling factors in the synthesis of cucurbituril and its homologues. *Org Chem* 66:8094
30. Kim J, Jung IS, Kim SY, Lee E, Kang JK, Sakamoto S, Yamaguchi K, Kim K (2000) New cucurbituril homologues: syntheses, isolation, characterization, and X-ray crystal structures of cucurbit[*n*]uril (*n* = 5, 7, and 8). *J Am Chem Soc* 122:540
31. Lee JW, Samal S, Selvapalam N, Kim HJ, Kim K (2003) Cucurbituril homologues and derivatives: new opportunities in supramolecular chemistry. *Acc Chem Res* 36:621
32. Kim K (2002) Mechanically interlocked molecules incorporating cucurbituril and their supramolecular assemblies. *Chem Soc Rev* 31:96
33. Rekharsky MV, Ko YH, Selvapalam N, Kim K, Inoue Y (2007) Complexation thermodynamics of cucurbit[6]uril with aliphatic alcohols, amines, and diamines. *Supramol Chem* 19:39
34. Kim Y, Kim H, Ko YH, Selvapalam N, Rekharsky MV, Inoue Y, Kim K (2009) Complexation of aliphatic ammonium ions with a water-soluble cucurbit[6]uril derivative in pure water: isothermal calorimetric, NMR, and X-ray crystallographic study. *Chem Eur J* 15:6143
35. Kim K, Selvapalam N, Oh DH (2004) Cucurbiturils—a new family of host molecules. *J Incl Phenom Macrocycl Chem* 50:31
36. Park KM, Kim SY, Heo J, Whang D, Sakamoto S, Yamaguchi K, Kim K (2002) Synthetic molecular machine based on reversible end-to-interior and end-to-end loop formation triggered by electrochemical stimuli. *J Am Chem Soc* 124:2140
37. Kim K, Jeon WS, Kang JK, Lee JW, Jon SY, Kim T, Kim K (2003) A pseudorotaxane on gold: formation of self-assembled monolayers, reversible dethreading and rethreading of the ring, and ion-gating behavior. *Angew Chem* 115:2395
38. Kim J, Kim Y, Baek K, Ko YH, Kim D, Kim K (2008) Direct force measurement between cucurbit[6]uril and spermine using atomic force microscopy. *Tetrahedron* 64:8389
39. Whang DM, Park KM, Heo J, Ashton P, Kim K (1998) Molecular necklace: quantitative self-assembly of a cyclic oligorotaxane from nine molecules. *J Am Chem Soc* 120:4899
40. Lee ES, Heo JS, Kim K (2000) A three-dimensional polyrotaxane network. *Angew Chem Int Ed* 39:2699
41. Lee JW, Kim KP, Kim K (2001) A kinetically controlled molecular switch based on bistable [2]rotaxane. *Chem Commun* 11:1042
42. Tan YB, Choi SW, Lee JW, Ko YH, Kim K (2002) Synthesis and characterization of novel side-chain pseudopolyrotaxanes containing cucurbituril. *Macromolecules* 35:7161
43. Choi S, Lee JW, Ko YH, Kim K (2002) Pseudopolyrotaxanes made to order: cucurbituril threaded on polyviologen. *Macromolecules* 35:3526
44. Jeon WS, Ziganshina AY, Lee JW, Ko YH, Kang JK, Lee C, Kim K (2003) A [2]pseudorotaxane-based molecular machine: reversible formation of a molecular loop driven by electrochemical and photochemical stimuli. *Angew Chem Int Ed* 382(42):4097
45. Kim K, Jeon WS, Kang JK, Lee JW, Jon SY, Kim T (2003) A pseudorotaxane on gold: formation of self-assembled monolayers, reversible dethreading and rethreading of the ring, and ion-gating behavior. *Angew Chem Int Ed* 42:2293
46. Kim K, Kim D, Lee JW, Ko YH (2004) Growth of poly(pseudorotaxane) on gold using host-stabilized charge-transfer interaction. *Chem Commun* 7:848
47. Dybtsev DN, Chun H, Yoon SH, Kim D, Kim K (2004) Microporous manganese formate: a simple metal–organic porous material with high framework stability and highly selective gas sorption properties. *J Am Chem Soc* 126:32
48. Buschmann HJ, Meschke C, Schollmeyer E (1998) Cucurbituril as host molecule for the complexation of aliphatic alcohols, acids and nitriles in aqueous solution. *An Quim Int Ed* 94:241

49. Buschmann HJ, Jansen K, Schollmeyer E (1998) Thermodynamic data for complex formation between cucurbituril and alkali and alkaline earth cations in aqueous formic acid solution. *J Solution Chem* 27:135
50. Meschke C, Buschmann HJ, Schollmeyer E (1999) Polyrotaxanes and pseudopolyrotaxanes of polyamides and cucurbituril. *Polymer* 40:945
51. Buschmann HJ, Jansen K, Schollmeyer E (2000) Cucurbituril as host molecule for the complexation of aliphatic alcohols, acids and nitriles in aqueous solution. *Thermochim Acta* 346:33
52. Yamaguchi N, Gibson HW (2000) Non-covalent chemical modification of crown ether side chain polymethacrylates with a secondary ammonium salt: a new polypseudorotaxane. *Macromol Chem Phys* 201:815
53. Freitag M, Galoppini E (2010) Cucurbituril complexes of viologens bound to TiO<sub>2</sub> films. *Langmuir* 26:8262
54. Thangavel A, Rawashdeh A, Sotiriou-Leventis C, Leventis A (2009) Ultrafast asynchronous concerted excited-state intramolecular proton transfer and photodecarboxylation of *o*-acetylphenylacetic acid explored by combined CASPT2 and CASSCF studies. *Org Lett* 11:1595
55. Ogoshi T, Masuda K, Yamagishi T, Nakamoto Y (2009) Side-chain polypseudorotaxanes with heteromacrocyclic receptors of cyclodextrins (CDs) and cucurbit[7]uril (CB7): their contrast lower critical solution temperature behavior with  $\alpha$ -CD,  $\gamma$ -CD, and CB7. *Macromolecules* 42:8003
56. Mock WL (1995) Supramolecular chemistry II—host design and molecular recognition. *Top Curr Chem* 175:1
57. Kim C, Agasti S, Zhu Z, Isaacs L, Rotello V (2010) Host–guest chemistry inside the cell: recognition-mediated activation of therapeutic gold nanoparticles. *Nat Chem* 2:962
58. Lagona J, Mukhopadhyay P, Chakrabarti S, Isaacs L (2005) The cucurbit[*n*]uril family. *Angew Chem* 117:4922
59. Mukhopadhyay P, Zavalij PY, Isaacs L (2006) High fidelity kinetic self-sorting in multi-component systems based on guests with multiple binding epitopes. *J Am Chem Soc* 128:14093
60. Isaacs L (2009) Cucurbit[*n*]urils: from mechanism to structure and function. *Chem Commun* 9:619
61. Phan A, Doonan CJ, Uribe-Romo FJ, Knobler CB, Keeffe MO, Yaghi OM (2010) Synthesis, structure, and carbon dioxide capture properties of zeolitic imidazolate frameworks. *Acc Chem Res* 43:58
62. Jiao D, Biedermann F, Tian F, Scherman OA (2010) A systems approach to controlling supramolecular architecture and emergent solution properties via host–guest complexation in water. *J Am Chem Soc* 132:15734
63. Yang H, Tan YB, Wang YX (2009) Fabrication and properties of cucurbit[6]uril induced thermo-responsive supramolecular hydrogels. *Soft Matter* 5:3511
64. Hou ZS, Tan YB, Huang YL, Zhang Y, Zhou QF (2005) Synthesis and characterization of side-chain pseudopolyrotaxanes by supramolecular self-assembly of cucurbituril[6] and poly(4-vinyl-*N*-butyryridinium bromide). *Acta Polym Sin* 4:491
65. Hou ZS, Tan YB, Kim K, Zhou QF (2006) Synthesis, characterization and properties of side-chain pseudopolyrotaxanes consisting of cucurbituril[6] and poly-N1-(4-vinylbenzyl)-1,4-diaminobutane dihydrochloride. *Polymer* 47:742
66. Hou ZS, Tan YB, Zhou QF (2006) Side-chain pseudopolyrotaxanes by threading cucurbituril[6] onto quaternized poly-4-vinylpyridine derivative: synthesis and properties. *Polymer* 47:5267
67. Huang XL, Tan YB, Wang YX, Yang H, Cao J, Che YJ (2008) Synthesis, characterization, and properties of copolymer of acrylamide and complex pseudorotaxane monomer consisting of cucurbit[6]uril with butyl ammonium methacrylate. *J Polym Sci A* 46:5999
68. Yang H, Tan YB, Hao JC (2010) Side-chain polypseudorotaxanes by threading cucurbit[7]uril onto poly-*N*-*n*-butyl-*N'*-(4-vinylbenzyl)-4,4'-bipyridinium bromide chloride: synthesis, characterization, and properties. *J Polym Sci A* 48:2135
69. Yang H, Tan YB, Hao JC (2011) Cucurbit[7]uril moving on side chains of polypseudorotaxanes: synthesis, characterization and properties. *J Polym Sci A* 49:2138
70. Dhara D, Chatterji PR (2000) Swelling and deswelling pathways in non-ionic poly(*N*-isopropylacrylamide) hydrogels in presence of additives. *Polymer* 41:6133
71. Kakinoki S, Kaetsu I, Nakayama M, Sutani K, Uchida K, Yukutake K (2003) Temperature and pH responsiveness of poly-(DMAA-*co*-unsaturated carboxylic acid) hydrogels synthesized by UV-irradiation. *Radiat Phys Chem* 67:685

72. Haraguchi K, Farnworth R, Ohbayashi A, Takehisa T (2003) Compositional effects on mechanical properties of nanocomposite hydrogels composed of poly(*N,N*-dimethylacrylamide) and clay. *Macromolecules* 36:5732
73. Lin Z, Cheng Y, Lv H, Zhang L, Yang B (2010) Preparation and characterization of novel ZnS/sulfur-containing polymer nanocomposite optical materials with high refractive index and high nanophase contents. *Polymer* 51:5424
74. Debye P (1947) Molecular-weight determination by light scattering. *J Phys Colloid Chem* 51:18
75. Zimm BH (1948) The scattering of light and the radial distribution function of high polymer solutions. *J Chem Phys* 16:1099
76. Li YB, Chen XD, Zhang MQ, Luo WA, Yang J, Zhu FM (2008) Macromolecular aggregation of aqueous polyacrylic acid in the presence of surfactants revealed by resonance Rayleigh scattering. *Macromolecules* 41:4873
77. Buschman HJ, Cleve E, Schollmeyer E (1992) Cucurbituril as a ligand for the complexation of cations in aqueous solutions. *Inorg Chim Acta* 193:93
78. Siegal R, Firestone B (1988) pH-dependent equilibrium swelling properties of hydrophobic polyelectrolyte copolymer gels. *Macromolecules* 21:3254
79. Liu N, Yi M, Ahai M, Li J, Ha H (2001) Radiation synthesis and characterization of polyDMAEMA hydrogel. *Radiat Phys Chem* 61:69
80. Chen YF, Yi M (2001) Swelling kinetics and stimuli-responsiveness of poly(DMAEMA) hydrogels prepared by UV-irradiation. *Radiat Phys Chem* 61:65